Title
Posttraumatic Reduction of Edema with Aquaporin-4 RNA Interference Improves Acute and Chronic Functional Recovery

Journal
Cerebrovascular and Brain Metabolism Reviews, 33(10)

ISSN
1040-8827

Authors
Fukuda, Andrew M
Adami, Arash
Pop, Viorela
et al.

Publication Date
2013-10-01

DOI
10.1038/jcbfm.2013.118

Peer reviewed

Journal of Cerebral Blood Flow & Metabolism (2013) 33, 1621–1632

www.jcbfm.com

ORIGINAL ARTICLE

Posttraumatic reduction of edema with aquaporin-4 RNA interference improves acute and chronic functional recovery

Andrew M Fukuda[1,2,5], Arash Adami[3,5], Viorela Pop[2], John A Bellone[4], Jacqueline S Coats[2], Richard E Hartman[4], Stephen Ashwal[3], Andre Obenaus[2,3] and Jerome Badaut[1,2]

Traumatic brain injury (TBI) is common in young children and adolescents and is associated with long-term disability and mortality. The neuropathologic sequelae that result from juvenile TBI are a complex cascade of events that include edema formation and brain swelling. Brain aquaporin-4 (AQP4) has a key role in edema formation. Thus, development of novel treatments targeting AQP4 to reduce edema could lessen the neuropathologic sequelae. We hypothesized that inhibiting AQP4 expression by injection of small-interfering RNA (siRNA) targeting AQP4 (siAQP4) after juvenile TBI would decrease edema formation, neuroinflammation, neuronal cell death, and improve neurologic outcomes. The siAQP4 or a RNA-induced silencing complex (RISC)-free control siRNA (siGLO) was injected lateral to the trauma site after controlled cortical impact in postnatal day 17 rats. Magnetic resonance imaging, neurologic testing, and immunohistochemistry were performed to assess outcomes. Pups treated with siAQP4 showed acute (3 days after injury) improvements in motor function and in spatial memory at long term (60 days after injury) compared with siGLO-treated animals. These improvements were associated with decreased edema formation, increased microglial activation, decreased blood–brain barrier disruption, reduced astrogliosis and neuronal cell death. The effectiveness of our treatment paradigm was associated with a 30% decrease in AQP4 expression at the injection site.

Journal of Cerebral Blood Flow & Metabolism (2013) **33,** 1621–1632; doi:10.1038/jcbfm.2013.118; published online 31 July 2013

Keywords: aquaporin; astrocyte; juvenile traumatic brain injury; pediatric neurology; siRNA

INTRODUCTION

Traumatic brain injury (TBI) affects ~1.7 million people annually and contributes to 30% of all injury-related deaths in the United States. An important subgroup is injured children (aged 0 to 14 years) of which a half million require treatment in local emergency departments.[1] Despite this increasing incidence of juvenile TBI (jTBI), there are currently no effective pharmacological treatments.

Traumatic brain injury is divided into two main types of injuries: primary injuries due to a direct and immediate mechanical disruption of brain tissue; and secondary injuries, a matrix of delayed events affecting neuronal, glial, and vascular structures.[2] The severity of primary injuries has decreased in recent years due to increased public and legislative awareness concerning preventative measures such as regulation of motor vehicle speed limits and wearing protective helmets during competitive sport activities. Thus, development of effective postinjury treatments should focus on targeting secondary injury cascades. This is especially important in jTBI because the brain is still undergoing development and secondary injuries are more severe in the pediatric than in adult population with long-lasting cognitive, emotional, and motor effects.[3] Secondary injuries including blood–brain barrier (BBB) disruption and edema formation are pathologic hallmarks after jTBI and contribute to the myriad of long-lasting consequences of jTBI,[4] and make excellent clinical targets for improving outcome. We recently characterized the behavioral changes, brain tissue properties, as well as neurovascular unit transformation up to 60 days after a controlled cortical impact (CCI) in juvenile rats (postnatal 17 days old).[5–7]

Aquaporin-4 (AQP4) is mainly expressed in perivascular astrocytic endfeet and is the most abundant brain aquaporin and has been shown to have a central role in edema formation in several cerebrovascular diseases.[8] However, the beneficial or deleterious role of AQP4 in edema formation remains unclear and depends on the pathologic model.[9] We recently showed an increase in edema formation at 1 and 3 days after injury with concomitant decreased apparent diffusion coefficient (ADC) and increased T2 values in a model of jTBI.[6] These magnetic resonance imaging (MRI) changes were associated with increase in the AQP4 expression at 3 days, suggesting a central role of AQP4 in edema formation in jTBI.[6] Nonetheless, several studies using AQP4 knockout mice have shown significant decreases in edema formation in several injury models, including adult TBI.[10] Despite several recent reports proposing the use of ionic channel inhibitors to block AQP4 channels[11] and pretreatment with certain drugs,[12] there are no specific AQP inhibitors available for clinical use.[8] Recently, small interfering RNA (siRNA) to transiently knockdown proteins of interest has garnered considerable translational attention with improvements noted in clinical trials using siRNA against vascular

[1]Department of Physiology, Loma Linda University, Loma Linda, California, USA; [2]Department of Pediatrics, Loma Linda University Medical Center, Loma Linda, California, USA; [3]Department of Neuroscience, University of California, Riverside, California, USA and [4]Department of Psychology, Loma Linda University Loma Linda, California, USA. Correspondence: Dr J Badaut, Departments of Pediatrics and Physiology, Loma Linda University School of Medicine, Coleman Pavilion, Room A1120, 11175 Campus Street, Loma Linda, CA 92354, USA.
E-mail: jbadaut@llu.edu
This study was supported by a grant from the National Institute of child disorders (NICHD) R01HD061946 and The Swiss National Science Foundation (Jerome Badaut). A portion of this material was performed in the Loma Linda University School of Medicine Advanced Imaging and Microscopy Core (LLUSM AIM) that is supported by the National Science Foundation under Major Research Instrumentation, Division of Biological Infrastructure Grant No. 0923559 (Sean M Wilson) and the Loma Linda University School of Medicine.
[5]These two authors contributed equally to this work.
Received 25 January 2013; revised 30 April 2013; accepted 10 June 2013; published online 31 July 2013

endothelial growth factor receptors for the treatment of cancer.[13] In our group, we have recently shown that siRNA against AQP4 (siAQP4) can effectively reduce brain AQP4 expression *in vitro* and *in vivo*.[14] In the present study, we hypothesized that using siAQP4 injection as a treatment to decrease AQP4 expression after CCI in juvenile rats would decrease edema formation, BBB disruption, and neuroinflammation (astrogliosis and microglia activation) as well as improve neurologic outcomes.

MATERIALS AND METHODS

Animals

The manuscript was written in accordance with the ARRIVE guidelines. Experiments and care of animals were conducted according to the principles and procedures of the Guidelines for Care and Use of Experimental Animals and were approved by the Loma Linda University Institutional Review Board. Sprague Dawley rat pups at postnatal day 17 (P17) were housed in a temperature-controlled (22°C to 25°C) animal facility on a 12-hour light/dark cycle 7 days before the surgery.

Small Interfering RNA preparation. An *in vivo* AQP4 silencing protocol was adapted as described in our previous studies.[14] Briefly, SMART-pool containing four siRNA duplexes against AQP4 (400 ng, siAQP4; Dharmacon Research, Lafayette, CO, USA) and non targeting siRNA (siGLO RISC-free-control-siRNA, Dharmacon Research) were mixed with interferin (Polypus Transfection, Illkirch, France) diluted in a saline solution (0.9%) containing 5% glucose for a final volume of 5 μL and incubated on ice for 20 minutes before injection.

Controlled Cortical Impact Injury and Small-Interfering RNA Injection

Controlled cortical impact was performed in P17 rat pups as previously described.[5] Rats were anesthetized with isoflurane (2%) and placed in a stereotaxic apparatus (David Kopf Instrument, Tujunga, CA, USA) where a 5-mm diameter craniotomy was performed over the right hemisphere at 3 mm posterior from the bregma and 4 mm lateral to the midline. Animals were subjected to a CCI with a 2.7 mm round tip angled 20° at a velocity of 6 m/s to a depth of 1.5 mm below the cortical surface using an electromagnetic impactor (Leica, Richmond, IL, USA). After craniotomy, the dura was intact in both groups and after induction of TBI none of the animals in the siGLO or siAQP4 groups had major bleeding or herniation of cortical tissues.

Injection of siRNA was performed 10 minutes after the injury lateral to the site of the impact using a 30-gauge needle on a Hamilton syringe (3 mm posterior to bregma, 6 mm lateral to midline, and 1.0 mm below cortical surface). The syringe was attached to a nanoinjector (Leica) and a volume of 4 μL of siRNA was infused at a rate of 0.4 μL/min. After suturing, all pups received an intraperitoneal injection of buprenorphine (0.01 mg/kg; Tyco Healthcare Group LP, Mansfield, MA, USA) for pain relief and then placed on a warm heating pad for recovery before being returned to their dams. A second siRNA injection was repeated 2 days later in all pups using the same injection protocol. Total number of animals used for the study was 27 rats divided in $n = 15$ rats for siGLO and $n = 12$ for siAQP4 group.

Magnetic Resonance Imaging

Magnetic resonance imaging was performed at 1 and 3 days. Pups were lightly anesthetized using isoflurane (1.0%) and imaged on a Bruker Avance 11.7 T (Bruker Biospin, Billerica, MA, USA).[15] Two imaging data sets were acquired: (1) a 10 echo T2 and (2) a diffusion weighted imaging sequence in which each sequence collected 20 coronal slices (1 mm thickness and interleaved by 1 mm). The 11.7T T2 sequence had the following parameters: repetition time/echo time = 2,357.9/10.2 ms, matrix = 128 × 128, field of view = 2 cm, and 2 averages. The diffusion-weighted imaging sequence had the following parameters: repetition time/echo time = 1,096.5/50 ms, two *b* values (116.960, 1,044.422 s/mm^2), matrix = 128 × 128, field of view = 2 cm, and 2 averages.

Region of Interest and Volumetric Analysis

T2 and ADC values were quantified using previously published standard protocols.[14] Regions of interest (ROIs) were placed on the imaging section with the maximally detected injury using Cheshire (Parexel International Corp., Waltham, MA, USA). Lesion and ipsilateral hippocampus were delineated on T2 images and overlaid onto corresponding T2 and ADC maps. The mean, standard deviation, and area for each ROI were extracted.

Behavioral Testing

The behavioral evaluation was performed on two independent sets of animals. Foot-fault and rotarod testing was performed at 1, 3, 7, and 60 days, where the foot-fault test evaluated sensorimotor and proprioception while the rotarod test evaluated sensorimotor coordination as previously reported in our earlier studies.[5] All tests at each time point were performed on siGLO- and siAQP4-treated jTBI rats within a 3-hour morning time block (0800 to 1100 h). The siGLO- and siAQP4-treated jTBI rats were interleaved in testing sequence. To further control potential confounds, the same tests were administered in the same order at all of the time points, by the same investigators (AA, VP, and JC) blinded to the experimental groups. For the behavioral tests, the videos and extraction of the data were performed by JB and RH, who were also blinded to the experimental groups.

Foot-fault testing was performed on an elevated platform (50 cm × 155 cm; ClosetMaid, Ocala, FL, USA) with parallel wire bars 1.5 cm apart and raised 100 cm above the floor at 1, 3, 7, and 60 days. Rats were placed in the middle of the platform and the movements were video-recorded for a period of 60 seconds in two separate trials, 30 minutes apart. When a rodent's paw (fore- or hind-limb) slipped completely through the parallel bar, it was considered as an individual fault. The average foot-fault score was calculated from the total number of faults from two 60-second trials.

Rotarod evaluation was performed on all the animals at 1, 3, 7, and 60 days (SD Instruments, San Diego, CA, USA). A rotating 7-cm-wide spindle with a continuous speed (20 RPM) was used to evaluate performance during two trials (15 minutes apart). Latency to fall was recorded as a measure of motor coordination and balance. The maximum time spent on the test was 60 seconds, if the rat did not fall. The two fall latencies were summed and express in total time (s) for two trials.

At 60 days after injury a battery of tests were performed over 4 days to evaluate the overall cognitive performance of the animals including open field, zero maze, and Morris Water Maze (MWM).[5] (1) Open field was used to assess the overall locomotor activity in a plastic box (50 × 36 × 45 cm), and each rat was monitored for 30 minutes with an overhead video camera using Noldus Ethovision software (Tacoma, WA, USA). The total distance traveled by each rat was recorded.[5] (2) On day 2, the elevated zero maze tests used an elevated circular track of 10 cm wide with a 100-cm outer diameter and two sets of 30 cm high walls enclosing two opposing quadrants of the track, leaving the other two opposing quadrants open and brightly lit. This test was used to evaluate anxiety-like behavior by a 5-minute observation, and the outcome measure was the percentage of time spent in the enclosed (dark) half of the maze. (3) Finally, the MWM test was performed to assess spatial learning and memory in the rats. The test consists of a tank 100 cm in diameter, filled with opaque water and an 11-cm diameter escape platform was placed. Recording the animal with an overhead camera and the Noldus Ethovision system allowed for assessment of variables such as swim distance, swim speed, and relative angular velocity (left/right turn bias). The first day of testing consisted of the cued learning paradigm, designed to test for nonassociative factors that could affect the scoring on the MWM, such as motivation, swimming ability, and vision. The platform was visible by protruding 2 cm above the waterline with a 40-cm wooden rod attached. Animals were placed in the tank and required to simply swim to the visible platform to end the task. Each animal completed 10 trials consisting of 5 blocks of 2 trials each, with their starting location and that of the platform being shifted throughout the task. If the rat had not found the platform after 60 seconds, then it was guided to the platform, where it remained for 5 seconds. The swim path was recorded and each animal's total swim distance was determined for each trial. Day 2 and 3 of the MWM are the spatial paradigm designed to measure an animal's ability to learn and remember a hidden platform's location in the tank. During this paradigm, the platform is submerged ~2 cm below the water's surface, and release points varied throughout each day although the platform remained stationary. As in the cued paradigm, animals were required to swim to the platform to end the task. Unlike the cued paradigm, hiding the platform's surface under the water's surface required animals to learn and navigate to the location using spatial cues. Each animal completed 10 trials consisting of 5 blocks of 2 trials each. If the animal had not found the platform after 60 seconds, then it was

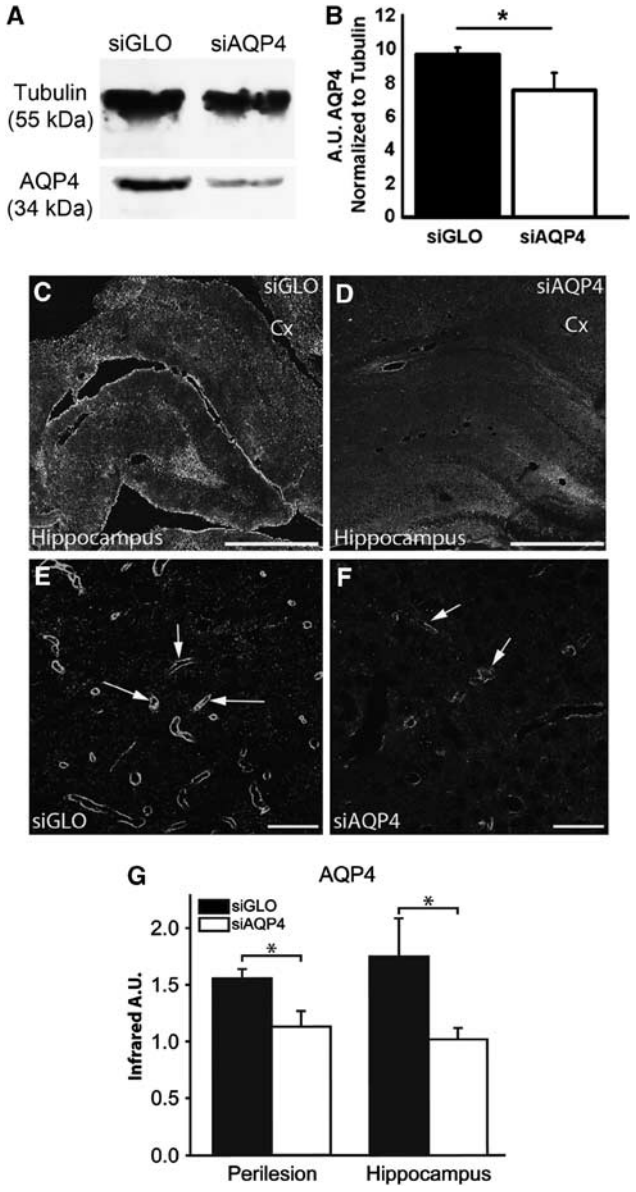

Figure 1. Reduced expression of aquaporin 4 (AQP4) after small-interfering RNA (siRNA) targeting AQP4 (siAQP4) injection. AQP4 western blot from adjacent PFA-fixed sections in siGLO and siAQP4 groups showed a band at around 34 kDa, with a decrease in the intensity in siAQP4-treated group. Tubulin was used to normalize the loading. The quantification of the intensity of the band showed a significant decrease in AQP4 ($P<0.05$). Representative images of AQP4 immunoreactivity in the cortical perilesion and hippocampus adjacent to the juvenile traumatic brain injury (jTBI) cavity (*) in siGLO- (**C**) and siAQP4-treated animals (**D**) at low magnification. AQP4 staining bordering the cavity is decreased in the siAQP4 (**D**) compared with the siGLO-treated animals (**C**) at day 3 after injury. Similarly, the AQP4 immunoreactivity is increased in the ipsilateral hippocampus of siGLO group (**C**) compared with siAQP4-treated animals (**D**). At higher magnification in perilesional cortex (Cx), AQP4 staining is predominant on astrocyte endfeet in contact with blood vessels (arrows, as previously described[16]) in siGLO (**E**) and siAQP4 (**F**) animals, with decreased staining of AQP4 in the siAQP4 group. This suggests that the siAQP4 treatment after jTBI prevents the increase in AQP4 expression on astrocyte endfeet. (**G**) AQP4 immunoreactivity was quantified and confirmed a significant decrease in AQP4 immunoreactivity in the siAQP4 compared with siGLO-treated rats in both the perilesional cortex and ipsilateral hippocampus (*$P<0.05$). Taken together, after jTBI, siAQP4 injection induced a decrease in AQP4 immunoreactivity acutely. Abbreviation: Cx, cortex; PFA, paraformaldehyde; scale bars (**C**, **D**) = 1 mm; (**E**, **F**) = 100 μm.

guided to and placed on the platform, where it remained for 5 seconds. The dependent variable for the spatial task was cumulative distance to the platform, a variable sensitive to both distance and time defined as a cumulative total of an animal's distance from the platform as measured 5 times every second. After each day of spatial testing, a probe trial was administered to measure an animal's ability to remember the platform's location. This trial was administered 1 hour after the final spatial trial of the day. The platform was removed and the animals were allowed to search the tank for 60 seconds. Dependent variables for this task included the number of times an animal entered the platform's previous location and percent time spent in the target quadrant.

Immunohistochemistry and Image Analysis

At 3 days, the animals were transcardially perfused with 4% paraformaldehyde, the brains were extracted and put in 30% sucrose for 48 hours and then stored in -22°C. Coronal sections were cut at 20 μm thickness at -22°C on a cryostat (Leica) and mounted on slides for immunohistochemical analysis.[14–16]

For immunoglobulin G (IgG) extravasation immunohistochemistry, sections were washed with phosphate-buffered saline (PBS), blocked with 1% bovine serum albumin in PBS, then incubated for 2 hours at room temperature with IRDye 800 conjugated affinity purified goat-anti-rat IgG (1:500; Rockland, Gilbertsville, PA, USA) in PBS containing 0.1% Triton X-100 and 1% bovine serum albumin. After washing, sections were scanned on an infrared (IR) scanner (Odyssey, Lincoln, NE, USA) to quantify fluorescence for the different ROIs as previously described.[14] Additional immunostaining was performed for rabbit polyclonal antibodies for AQP4 (1:300; Alpha Diagnostic, Owings Mill, MD, USA), chicken polyclonal antibodies for glial fibrillary acidic protein (GFAP, 1:500; Millipore, Billerica, MA, USA), mouse monoclonal antibodies for endothelial brain antigen (EBA, 1:1,000; Covance, Princeton, NJ, USA), mouse monoclonal antibodies for Neuronal Nuclei (NeuN, 1:200; Abcam, Cambridge, MA, USA), rabbit polyclonal antibodies for ionized calcium-binding adapter molecule (Iba-1, 1:300; Wako, Richmond, VA, USA), and mouse monoclonal antibodies for Claudin-5 (1:200; Invitrogen, Carlsbad, CA, USA) were used. Sections were washed with PBS, blocked with 1% bovine serum albumin in PBS, incubated with the respective primary antibodies overnight, then incubated with affinity purified secondaries conjugated to the desired wavelength either to be scanned on an IR scanner or to be observed under a confocal microscope (Olympus, BX41, Center Valley, PA, USA). All image acquisition parameters for the same proteins were kept constant for all of the animals for analysis and visualization purposes. All analysis was performed in a nonbiased, blinded manner. Aquaporin 4, GFAP, Claudin-5, and Iba-1 were quantified in a similar manner to IgG-extravasation staining as published previously.[14] In detail, slides were incubated with secondaries conjugated to the IR wavelength of either 680 or 800 nm. These slides were then scanned on an IR scanner (Odyssey), where images were saved with resolution of 21 μm per pixel. Three identical circular ROIs were drawn in the perilesional cortex (Figure 3A) at three different bregma levels (-1.40 mm, -2.56 mm, and -3.80 mm): the bregma level where lesion area was largest, one slice anterior and one posterior, for a total of nine ROIs per animal. The average fluorescence of these ROIs was calculated. The EBA and NeuN staining was quantified using the Mercator software (Explora-Nova, La Rochelle, France). The area of EBA staining was measured by drawing an ROI on the acquired image with the largest legion as determined and confirmed by MRI, and the total area of EBA-positive staining was determined and that value was divided by the area of the ROI. Thus, the percent of staining per given area was determined for each animal. Neuronal Nuclei-positive cells were counted on images acquired using constant parameters: i.e., the same values of the contrast, gain, and brightness were used. Similarly to EBA analysis, the tissue section with the largest legion was selected and the NeuN-positive cells were counted in an automated manner via the Mercator software and the density was determined. Microglial activation was quantified by calculating the average form factor ($FF = 4\pi \times \text{area}/\text{perimeter}^2$ of each cell) from the Iba-1-positive cells using the image software, MorphoPro (Explora-Nova, La Rochelle, France) on images acquired using constant parameters: i.e., the same values of the contrast, gain, and brightness were used. Negative control staining where the primary antibody or secondary antibody was omitted showed no detectable labelling.

Brain Tissue Processing for Western Blotting

A Protein FFPE extraction kit (Qiagen, Hilden, Germany) was used to process perfused brain slices for western blotting as previously published.[7]

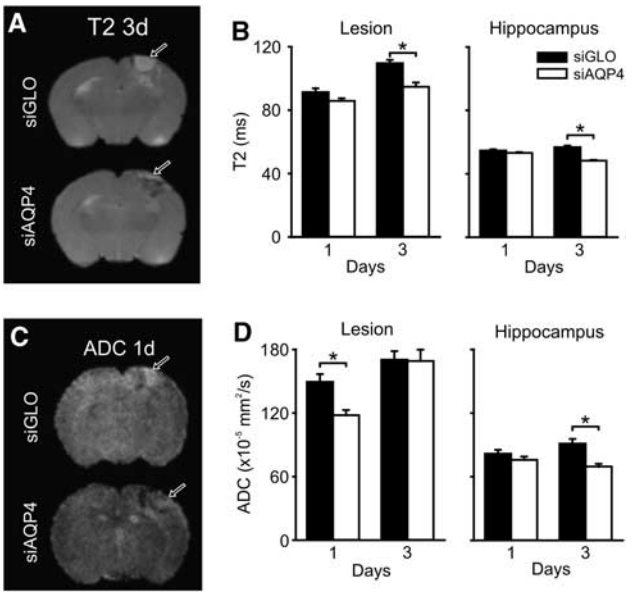

Figure 2. Quantitative neuroimaging of juvenile traumatic brain injury (jTBI) after small-interfering RNA (siRNA) targeting aquaporin 4 (siAQP4) treatment reveals decrements in edema. Representative T2 images at day 3 in siGLO- and siAQP4-treated pups show decreased edema at the lesion site after siAQP4 treatment (arrows) (**A**). siAQP4 pups had significantly decreased edema (*$P<0.001$) compared with siGLO pups within the lesion at day 3 (**B**). There was also a significant decrease in edema after siAQP4 treatment at day 3 within the hippocampus, ventral to the injury (*$P<0.001$) (**B**). Water mobility (apparent diffusion coefficients, ADC) was reduced in the siAQP4-treated pups (day 1 after injury, arrows) (**C**). Quantitative ADC revealed significantly decreased water mobility in siAQP4 pups in the lesion at 1 day after injury compared with siGLO (*$P<0.001$) (**D**). siAQP4 pups had significantly decreased ADC in the hippocampus at day 3, but not at 1 day (*$P<0.001$) (**D**). After jTBI, siAQP4 injection mitigated the edema formation associated with a decrease in the AQP4 (Figure 1).

Parietal cortical tissue around the lesion was excised from three coronal sections at bregma levels −1.40, −2.56, and −3.80 mm, which were adjacent to slices of interest used for immunohistochemistry quantification. Briefly, tissue was homogenized and processed according to kit instructions, and then samples were assayed for total protein concentration by bicinchoninic acid assay (Pierce Biotechnology Inc., Rockford, IL, USA). For gel electrophoresis, all samples were prepared with loading sample buffer and reducing agent (Invitrogen) for a total of 2 μg of rat protein loaded on a 4% to 12% SDS polyacrylamide gel (Nupage; Invitrogen). Proteins were transferred onto a polyvinylidene fluoride membrane (Perkin-Elmer, Schwerzenbach, Switzerland), blocked for 1 hour in Odyssey blocking buffer (LI COR Bio-Science, Lincoln, NE, USA), and incubated with a rabbit polyclonal anti-AQP4 (1:3,000; Alpha Diagnostic) and mouse anti-tubulin (1:10,000; Sigma-Aldrich Co., St Louis, MO, USA), and these blots were coincubated with goat anti-mouse secondary antibody coupled with Alexa-Fluor-800 (1:10,000; Rockland Immunochemicals, Gilbertsville, PA, USA) and goat anti-rabbit secondary antibody coupled with Alexa-Fluor-680 (1:10,000; Life Technologies: Molecular Probes, Grand Island, NY, USA) for 2 hours at room temperature. After PBS washes, the polyvinylidene fluoride membrane was visualized using the LI COR IR scanner and fluorescence activity was directly quantified Odyssey software (LI COR Bio-Science).

Statistics

The MRI and behavioral data were analyzed by two-way repeated measures analysis of variance with a *post hoc* Bonferroni test. One-way ANOVA was used for immunohistochemistry and western blot analysis. All data are expressed as the mean ± s.e.m.

RESULTS

Small-Interfering RNA Targeting Aquaporin 4 Treatment Reduces Aquaporin-4 Expression Acutely

Injection of siAQP4 induced a 31% decrease ($P<0.05$) in the level of AQP4 expression at 3 days (Figures 1A and 1B). In support of the western blot results, siAQP4-treated rats showed a 27% decrease in AQP4 staining within the perilesional tissues around the cavity on the ipsilateral cortex as well as a 33% decrease in the ipsilateral hippocampus compared with siGLO-treated animals ($P<0.05$) (Figures 1C to 1G). This decrease in AQP4 staining after jTBI was of similar magnitude to that which we previously reported in normal (i.e., no jTBI) juvenile brain tissues after siAQP4 injection.[14] In contrast, western blot and immunohistochemistry analysis showed no differences in AQP4 expression between siGLO- and siAQP4-treated animals at 60 days (Figures 6A to 6C). No significant changes found in the contralateral cortex or hippocampus at 3 and 60 days (data not shown).

Small-Interfering RNA Targeting Aquaporin 4 Treatment Reduces Acute Edema Formation

As determined by 1- and 3-day MRI, we found decreased T2 (edema) and ADC (water mobility) values in siAQP4 compared with siGLO-treated pups (Figure 2), strongly suggesting that siAQP4 reduced edema formation. Whereas T2 values increased in the lesion/perilesion area of siGLO-treated rats they were decreased in siAQP4 pups from 1 to 3 days (22% in the lesion/perilesion and 15% in the ipsilateral hippocampus). Values of ADC were also decreased by 21% in the lesion/perilesion at 1 day ($P<0.005$) and by 24% in the ipsilateral hippocampus at 3 days ($P<0.001$) in the siAQP4 compared with siGLO-treated rats (Figure 2). Overall, the data suggest an association between the regions showing reduced AQP4 staining and reduced edema formation (T2) and improved tissue characteristics (ADC) (Figures 1 and 2).

Reduced Blood–Brain Barrier Disruption in Small-Interfering RNA Targeting Aquaporin-4-Treated Rat Pups

Edema formation (i.e., increased T2 values) also appeared to be associated with BBB disruption, which improved after siAQP4 treatment. Integrity of BBB was assessed with Claudin-5 (tight junction protein), EBA and IgG-extravasation staining in the perilesional cortex and ipsilateral-hippocampus (Figure 3). Less BBB disruption was also shown through decreased IgG-extravasation staining intensity by 30% around the site of the injury in the siAQP4 group ($P<0.05$) (Figures 3B to 3D). Associated with decreased IgG staining, a 31% increase in the area of EBA staining in siAQP4 rats was observed (Figures 3E to 3G). Similarly, Claudin-5 immunoreactivity was higher in the siAQP4-treated animals around the cavity (Figures 3H to 3J).

Reduced Astrogliosis, Increased Microglial Activation, and Increased Neuronal Survival in Small-Interfering RNA Targeting Aquaporin 4-Treated Rat Pups

The effects of siAQP4 on neuroinflammation were evaluated by measurement of astrogliosis with GFAP immunoreactivity (Figure 4) and microglia activation with Iba-1 staining (Figure 4). The GFAP staining intensity was decreased by 39% around the cavity and by 26% in the ipsilateral hippocampus of siAQP4-rat pups compared with the siGLO group ($P<0.05$, Figure 4). In contrast, we observed an increase in the number of activated microglial cells, showing amoeboid shapes with less ramifications in the lesion site characterized by higher calculated FF in siAQP4 compared with siGLO-treated rats (Figure 4). This observation was also supported by a higher intensity of Iba-1 staining, a specific marker of microglia, using IR analysis (Figure 4). No significant differences were observed in the ipsilateral hippocampus.

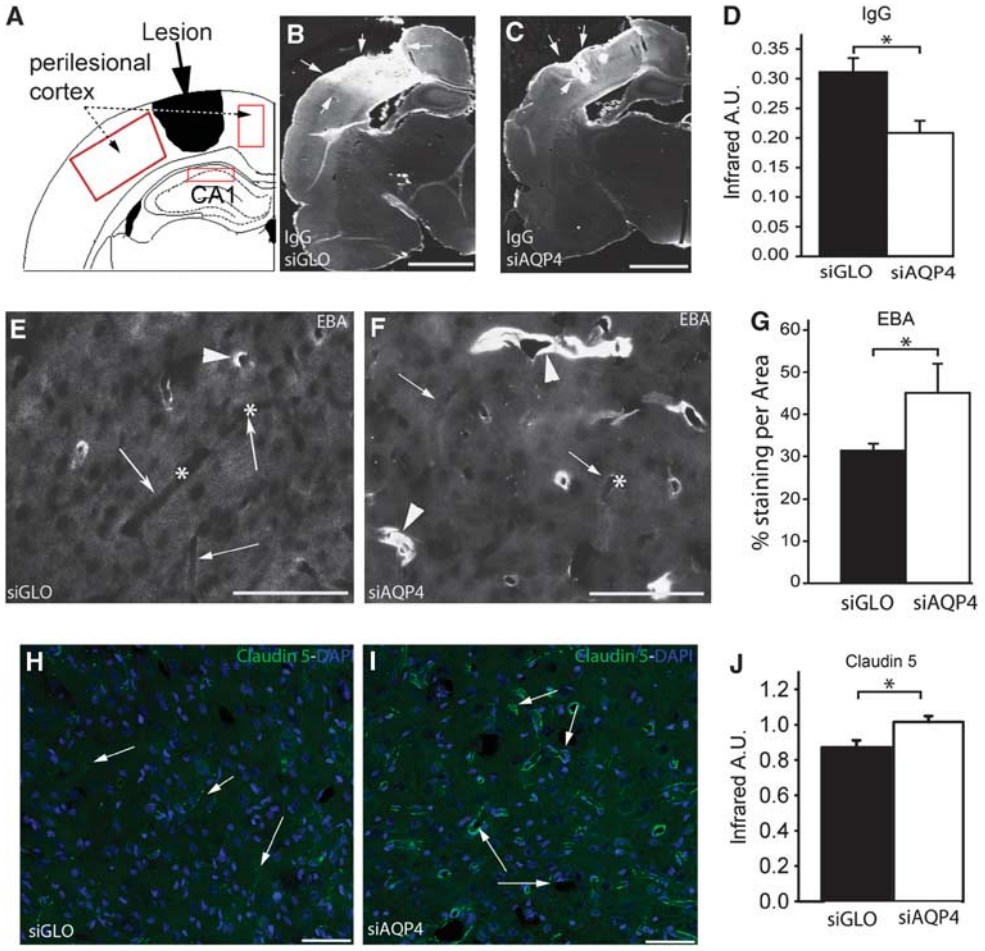

Figure 3. Small-interfering RNA (siRNA) targeting aquaporin 4 (siAQP4) treatment decreases blood–brain barrier (BBB) disruption after juvenile traumatic brain injury (jTBI). Drawing of the regions of interest (ROIs) used in the study to quantify protein and histologic changes in correlation with the magnetic resonance imaging (MRI) measurements (**A**). Representative photomicrographs of immunoglobulin (IgG)-extravasation immunofluorescence (arrows) in siGLO- (**B**) and siAQP4- (**C**) treated rat pups. siAQP4-treated rat pups showed significantly decreased IgG-extravasation staining adjacent to the lesion site compared with siGLO-treated animals ($^*P<0.05$), suggesting that the siAQP4 treatment mitigates BBB disruption (**D**). Endothelial barrier antigen (EBA) is a marker of intact endothelial cells in rats and disappears when the endothelial layer is disrupted. The arrows in (**E**) show blood vessels (asterisks) devoid of EBA staining in siGLO-treated animals. In contrast, siAQP4 rat pups had more EBA-positive staining (arrowheads) in the cortical perilesion tissue (**F**). Quantification of the EBA staining showed that the siAQP4-treated rat pups had more EBA-positive staining (arrowheads), suggesting decreased damaged blood vessels in the perilesion tissues ($^*P<0.05$) (**G**). This result is in accordance with the IgG-extravasation data showing improvement of the BBB after siAQP4 treatment (**A**–**C**). Similarly, Claudin-5 staining, a tight junction protein (in green **H**, **I**) showed increased staining in siAPQ4 (**I**, arrows) compared with siGLO-treated rats (**H**, arrows) and confirmed in the quantification of Claudin-5 immunoreactivity ($^*P<0.05$) (**J**). Increased levels of Claudin-5 suggest less BBB disruption consistent with decreased IgG-extravasation and increased EBA staining after siAQP4 treatment. Taken together, siAQP4 treatment results in less BBB disruption at day 3 after injury as seen by more tight junction proteins, more intact blood vessels, and less leakage of IgG from the peripheral blood vessels to brain tissue. Scale bars in panels **A**, **B** = 3 mm; **D**, **E** = 100 μm.

The effects of siAQP4 on neuronal survival were also measured by counting the number of NeuN-positive cells.[5,17] At 3 days, NeuN-positive cells were higher in the perilesional cortex adjacent to the cavity (62%) as well as in the ipsilateral hippocampus (56%) in the siAQP4 compared with siGLO-treated pups at 3 days (Figure 5).

At 60 days, there were no differences in AQP4 and GFAP staining (Figure 6A to 6C). No changes in microglial activation were observed at 60 days (Figure 6D). In contrast, there was a significantly higher number of NeuN-positive cells in the CA1 region of the ipsilateral hippocampus in siAQP4 animals compared with siGLO, however, no changes were observed in the ipsilateral cortex (Figures 6F, 6G, and 6I).

Improved Sensorimotor, Proprioception, and Spatial Memory After Small-Interfering RNA Targeting Aquaporin-4 Treatment

Concomitant with the observed decrease in edema and histologic improvements, motor functions were improved in siAQP4-treated rats. The siAQP4 pups had fewer foot faults at 1 and 3 days (respectively, 34% and 46%, $P<0.05$, Figure 7A). After 7 days, there were no more significant differences in the number of foot-faults (Figure 7A). Similarly, siAQP4-treated rats were able to stay on a rotarod 40% longer than siGLO-treated rat pups at 3 days (Figure 7B), that returned to baseline at 7 days after injury. Long-term improvements were tested up to 60 days after injury, with a battery of tests assessing several cognitive repertoires. The open field test did not show significant difference between the

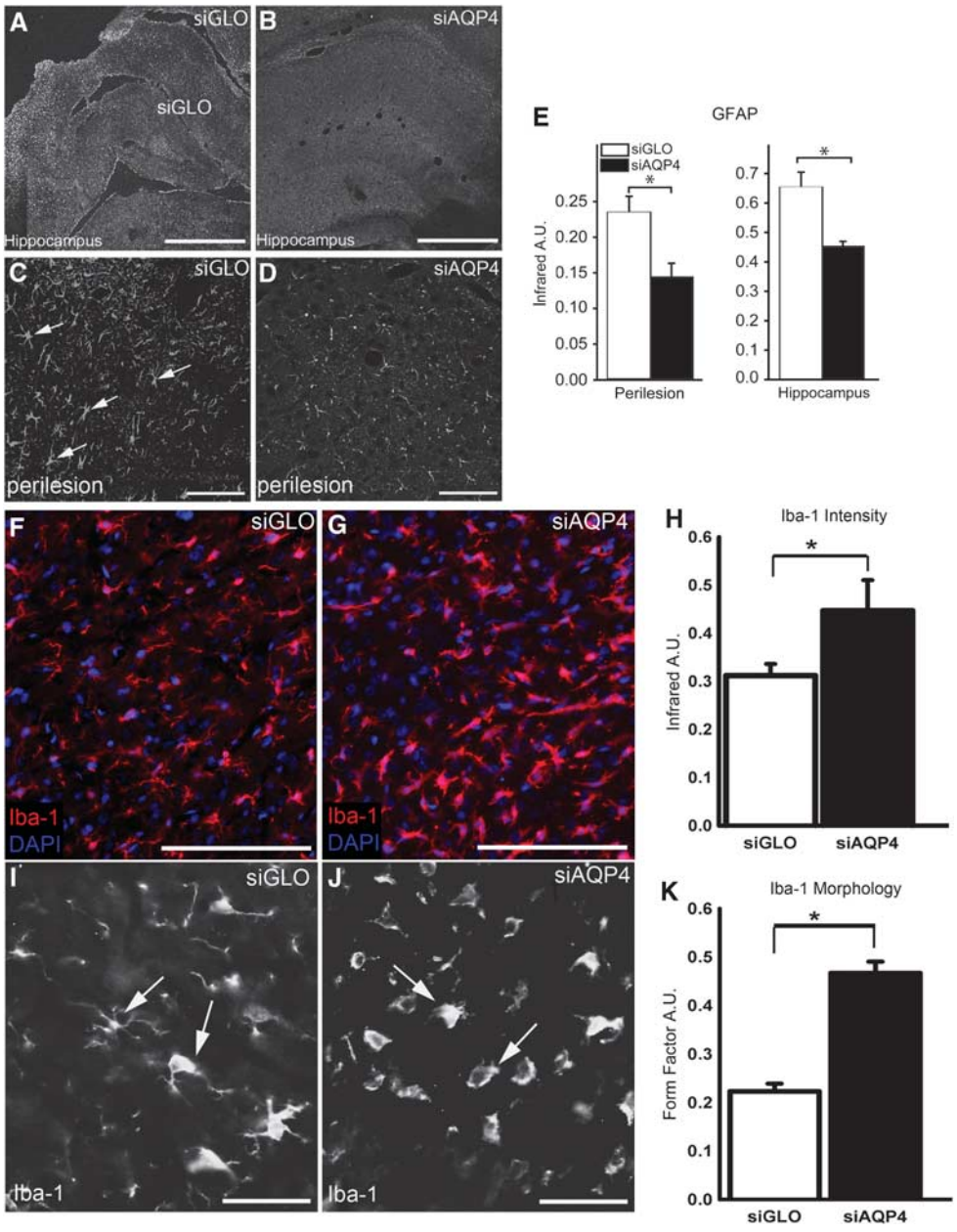

Figure 4. Small-interfering RNA (siRNA) targeting aquaporin-4 (siAQP4) treatment reduces astrogliosis and results in microglial activation acutely after juvenile traumatic brain injury (jTBI). Increased glial fibrillary acidic protein (GFAP) staining after injury is a marker of reactive astrocytes and astrogliosis associated with neuroinflammation. Representative images of regional GFAP immunoreactivity in the cortical perilesion in the siGLO- (**A**) and siAQP4-treated animals (**B**). GFAP staining in the region bordering the cavity (*) is decreased in the siAPQ4-treated rats compared with the siGLO-treated animals at day 3 after injury. Similarly in the hippocampus, the presence of GFAP staining in the reactive astrocytes in the siGLO-treated rats (**A**) is increased compared with siAQP4-treated animals (**B**). At higher magnification, increased GFAP-positive cells with swollen cell bodies and processes in the siGLO group (arrows, **C**) compared with siAQP4- (**D**) treated rats were observed in the perilesional cortex. The infrared intensity of the GFAP immunoreactivity was quantified and showed a significant decrease in GFAP staining in the siAQP4 compared with siGLO-treated rats in both the perilesional cortex and ipsilateral hippocampus (**E**) ($^*P < 0.05$). The significant decrease in GFAP in the siAQP4-treated rats suggests that siAQP4 treatment mitigates astrogliosis and the swelling of the astrocytes after jTBI. Immunoreactivity of Iba-1 (red), a specific marker of microglia, showed a higher intensity of staining in the siAQP4 group (**F**) compared with siGLO-treated rats (**G**). At higher magnification, Iba-1 staining presents different morphologic patterns between the two groups, suggesting that the microglia cells do not have the same level of activation. In the siGLO group (**I**), Iba-1-positive cells appear more ramified (arrows) and have less amoeboid-like shapes than microglial cells in siAQP4-treated rats (**J**, arrows). The amoeboid-like shapes observed for Iba-1-positive cells in the siAQP4-treated group (**J**, arrows) are associated with a more activated microglia phenotype. To quantify the morphologic differences, form factor (FF) analysis was performed where a higher FF correspond to a less ramified and more round cells, suggesting a more activated state for microglia. FF analysis revealed that siAQP4-treated rats had a significantly higher average FF compared with siGLO group (**K**) ($^*P < 0.01$) consistent with a more activated microglia in siAQP4 animals. Infrared analysis showed higher intensity fluorescence in the siAQP4 animals compared with siGLO at the lesion site (**H**) ($^*P < 0.05$). Scale bars in panels **A**, **B** = 1 mm; **C**, **D** = 100 μm, **F**, **G**, **I**, **J** = 20 μm.

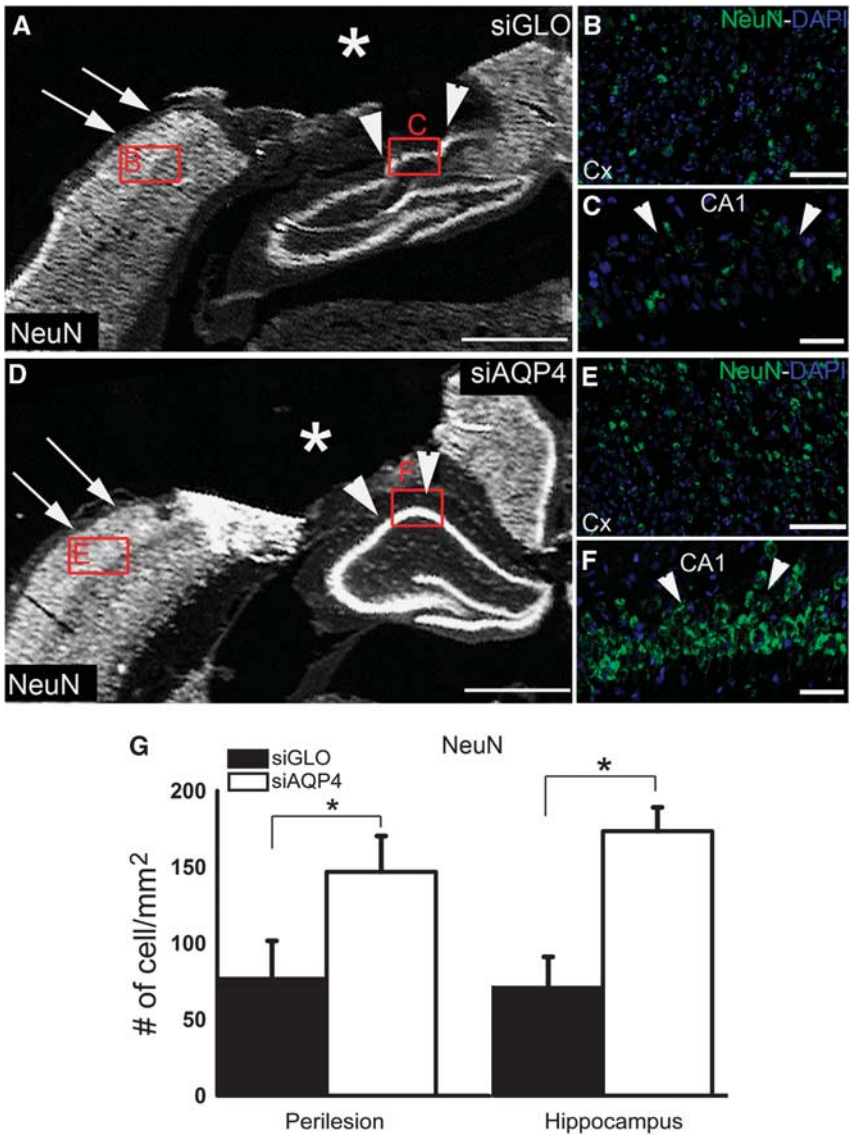

Figure 5. Small-interfering RNA (siRNA) targeting aquaporin-4 (siAQP4) treatment increases neuronal survival at 3 days after injury. NeuN (Neuronal Nuclei) stained sections show a higher staining in the siAQP4 animals (**D**–**F**) than the siGLO (**A**–**C**) in the cortex (**A**, **B**, **D**, **E**) and the hippocampus (**A**, **C**, **D**, **F**) adjacent to the cavity (*). Neuronal cell counts revealed a significant increase in the number of NeuN-positive cells (# of cell/mm^2) in both the perilesion (arrows, **A**, **D**) and hippocampus (arrowheads, **A**, **C**, **D**, **F**) of siAQP4 animals (**G**) (*$P<0.05$), suggesting improved neuronal survival after injury in siAQP4-treated rat pups compared with siGLO group. Scale bar **A**, **D** = 1.25 mm; **B**, **E** = 50 μm; **C**, **F** = 20 μm.

groups in overall locomotor activity (data not shown) and supported the MWM cued test showing no differences in the ability to swim (data not shown). Similarly, the zero maze tests did not show differences between the groups with the same time spent in the 'dark' quadrants (data not shown). During the spatial learning on the day 1 of the protocol, both groups were able to perform the task similarly (Figure 7C). However on the second day of the MWM protocol, when the platform is moved to a second location, siAQP4 animals spent more time than the nontreated group in trying to find the new location of the platform on the first block (Figure 7D). This suggests that siAQP4 animals have a better memory of the previous platform location and thus spent more time at the previous site (Figure 7E). These data are also supported by the probe test to assess the spatial memory. The siAQP4-treated rats spent significantly longer times than the siGLO group in the quadrant that previously contained the platform (Figure 7F). Improvement in spatial memory at 60 days after injury is associated with higher CA1 neuronal survival in siAQP4-treated group (Figure 6).

DISCUSSION

We report here for the first time that siAQP4 treatment is an effective mechanism for reducing edema after jTBI and improves functional recovery even up to 60 days after injury. Injection of siAQP4 reduced AQP4 expression by 30% and was associated with significant decrements in edema formation, less BBB disruption, decreased astrogliosis, increased microglia activation, reduced neuronal cell death as well as improved neurologic function during the acute phase after injury. We also observed that the siAQP4-treated animals had improved hippocampal neuronal cell cell counts and memory recall up to 60 days after injury as well. The uniqueness of our approach in implementing siRNA targeting of AQP4 to improve functional outcomes after jTBI at both short

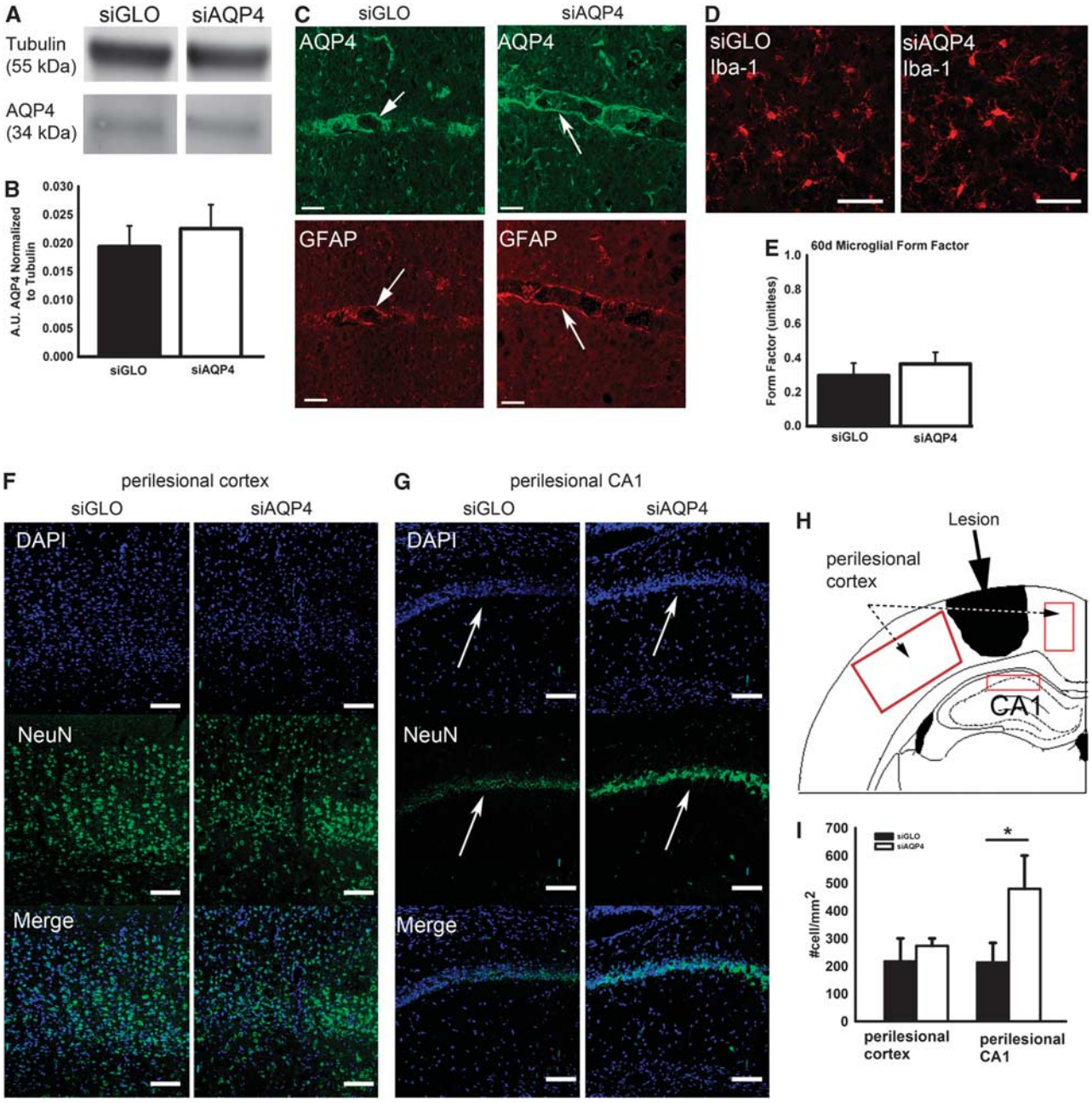

Figure 6. Small-interfering RNA (siRNA) targeting aquaporin-4 (siAQP4) treatment increases the neuronal survival in hippocampus at 60 days. At 60 days, AQP4 expression did not differ significantly between siAQP4 and siGLO as quantified via western blot (**A**, **B**). AQP4 and glial fibrillary acidic protein (GFAP) staining did not show overall obvious visible differences in staining intensity or staining pattern between the groups as shown in the exemplary confocal picture (**C**). The arrows represent penetrating arteries stained in both siGLO and siAQP4 (**C**). At 60 days, there were no visible differences in microglial staining visualized via Iba-1 immunohistochemistry between the siGLO and siAQP4 animals (**D**). Form factor analysis showed no significant differences between the animals, signifying no differences in microglial activation status (**E**). In the perilesional cortex of 60-day animals, Neuronal Nuclei (NeuN) cell count showed no significant differences (**F**, **I**). However, in the perilesional CA1 (arrow), siAQP4 animals had significantly higher number of NeuN-positive cells (**G**) ($^*P < 0.05$, **I**). A schematic drawing showing the regions of interest (in red) used to quantify NeuN numbers is shown (**H**). Scale bar **C**, **D** = 50 μm; **F**, **G** = 100 μm.

and long term time points after injury strongly suggests a potential future direction for clinical development.

Magnetic resonance imaging (T2, ADC) was used to temporally monitor edema formation as is performed clinically after brain injury.[8,18] Our MRI data showed less posttraumatic edema after siAQP4 treatment (Figure 2) as manifested by significantly reduced T2 values in siAQP4 compared with siGLO-treated rat pups at 3 days, suggesting less water accumulation within the lesion/perilesion and hippocampal tissues (Figure 2).

Beneficial effects of siAQP4 on water mobility as reflected by reduced ADC values were also observed. Values of ADC are dramatically increased in the injury site and likely correspond to cell death leading to an altered tissue matrix. This increase in ADC at the lesion is decreased in siAQP4 compared with siGLO-treated rats, suggesting that siAQP4 mitigates cell death at this early time point but not at 3 days (Figure 2). However, in adjacent tissues such as the hippocampus, the ADC values were also significantly decreased, suggesting that siAQP4 may prevent cell death even at

3 days in the hippocampus, by limiting edema expansion. This hypothesis is supported by the increased numbers of neurons in the siAQP4-treated animals at 3 days (Figure 6). However, decreased ADC could also be associated with a decrease in AQP4 expression on the astrocyte endfeet (Figure 1) at 3 days in accordance with our previous studies.[14] In fact, decreased AQP4

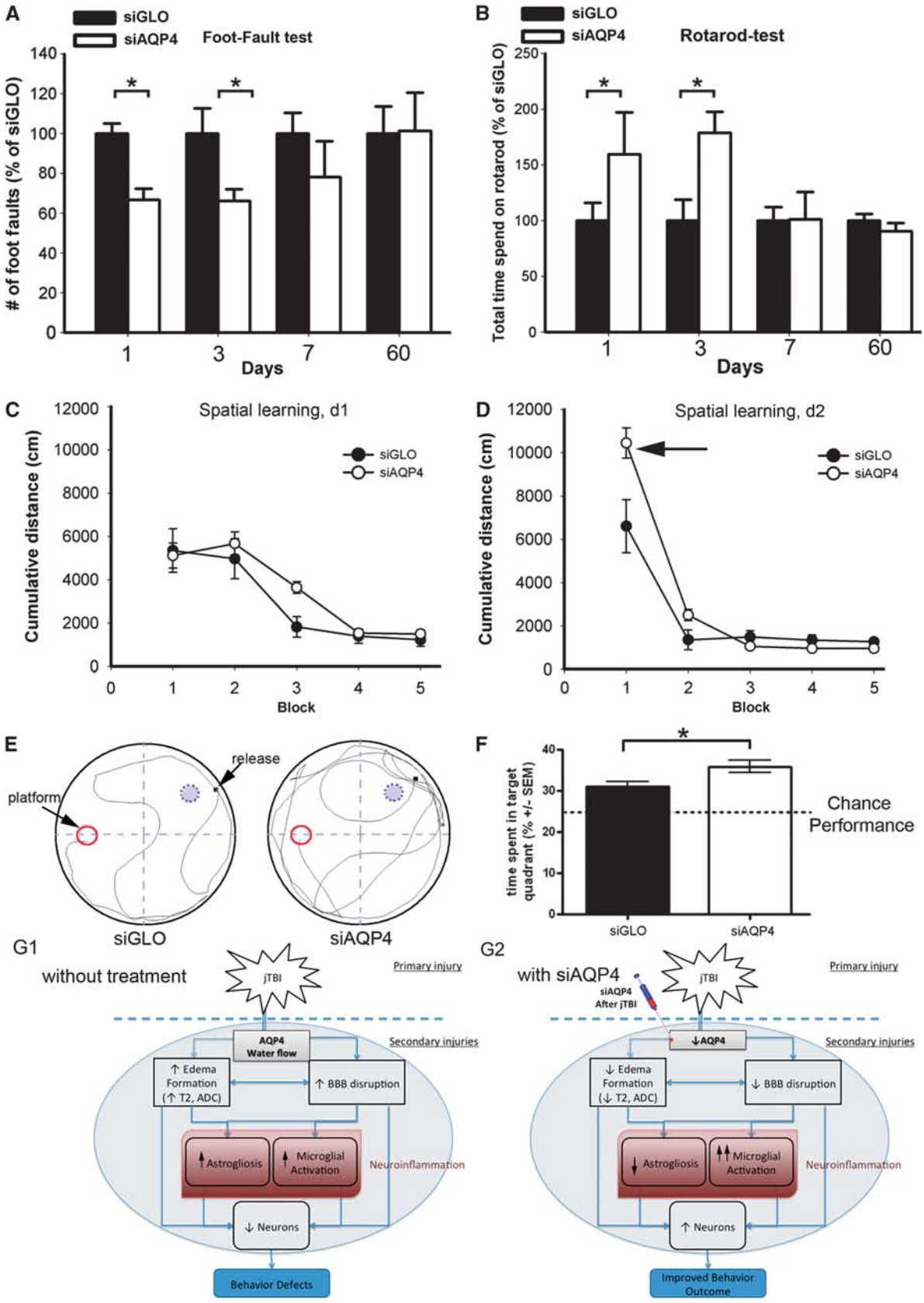

Figure 7. For legend see page 1630.

expression has been correlated with decreased ADC[14,19] and increased AQP4 expression has been correlated with increased ADC[20] in rats. This suggests that water diffusion is limited by the decrease in AQP4 in the siAQP4-treated pups (Figure 1). Together, the MRI data show that siAQP4 treatment prevents edema formation with decreased T2 and ADC values in the lesion and ipsilateral hippocampus. At 3 days, T2 values are significantly higher in the lesion/perilesion suggesting an increase in water content in the tissue due to ongoing vasogenic edema formation in the untreated animals, while the decrease in the siAQP4-treated rats suggests that siAQP4 prevents vasogenic edema formation. This hypothesis is supported by the evidence of less BBB disruption (decreased IgG extravasation, increased EBA and Claudin-5 staining) in siAQP4 compared with siGLO-treated animals. In fact, injection of siAQP4 after jTBI may prevent water entry into astrocytes and block subsequent swelling of these cells at 1 day as indicated by the lower values of ADC in siAQP4 animals compared with siGLO. Less osmotic stress on the astrocytes may prevent BBB disruption by maintenance of the physical and mechanical properties of the endothelial cells and also neurovascular unit (Figures 3 and 4). Therefore, less BBB disruption appears to be associated with less astrogliosis, which has been correlated with the severity of brain injury.[21]

The next question was whether beneficial effects could still be observed late after injury, and whether there was significant downregulation of AQP4. This is an important question when considering the hypothesized biphasic and dual role that AQP4 has, not only in edema formation, but also in edema clearance and maintaining regular water homeostasis.[22,23] It has been hypothesized and several experimental observations hint that the presence of AQP4 is detrimental acutely after injury because they contribute to the entry of water into the brain parenchyma so acute downregulation of AQP4 may be beneficial, but chronic AQP4 depletion may be detrimental as AQP4 is also needed for water clearance and maintenance of normal water homeostasis.[24–27] To this end, we performed a western blot at 60 days and also performed immunohistochemistry to see if there were visible differences in AQP4 expression levels. At 60 days, we observed no differences in AQP4 levels or staining. Thus injection of siAQP4 right after injury downregulates AQP4 acutely but does not lead to chronic, long-term depletion of AQP4. This is another beneficial effect of using siRNA as it allows conditional downregulation limited in the time of the target protein of interest.

The beneficial effects of siAQP4 treatment were also observed in the greater number of neurons (NeuN-positive cells) in siAQP4 compared with siGLO-treated rats at both acute and long term time points after. These improvements led to improved neurologic outcomes at 1 and 3 days in siAQP4-treated rats (Figure 7A and 7B). This improvement in motor function was not visible at 7 days, which may represent natural recovery or loss of some neurons in the perilesional cortex as shown at 60 days (Figure 6). Interestingly, at 60 days, there were a significantly greater number of NeuN-positive cells in the CA1 region of siAQP4 compared with siGLO; an effect which can be observed in memory improvement. Our unique data strongly suggest that the early decrease in AQP4 mitigates development of secondary injuries such as edema resulting in chronic neuroprotection for the perilesional structures, such as the hippocampus.

The siAQP4 treatment resulted in greater microglial activation around the injection site at 3 days but not at 60 days. Microglial activation after siAQP4 treatment is in accordance with previous observations in brain injury models using AQP4$^{-/-}$ mice.[28,29] However, acute microglial activation is hypothesized to be beneficial after injury,[30] whereas a chronic microglial activation is hypothesized to be detrimental,[30] so it is likely that at this time point, increased microglial activation due to siAQP4 treatment is contributing to the beneficial effects observed in our model. This observation suggests a potential relation between the level of AQP4 (Figure 1), astrogliosis, and microglia activation (Figures 4 and 7G1 andG2).

We have previously speculated in a previous review[23] two of the possible mechanisms responsible for the relationship between AQP4 and microglial activation. The first potential mechanism may be due to crosstalk that occurs between astrogliosis and microglial activation.[31] It is possible that the decreased extent of injury-induced reactive astrogliosis is a result of knocking down AQP4 resulting in increased microglial activity. A second possible mechanism behind the changes observed in posttraumatic microglial activation in response to injection of siRNA against AQP4 may be because of the stretch-activated chloride channels expressed in microglia cells.[32] Stretch-activated, also known as swelling-activated chloride channels, are activated by osmotic stress.[33] Activation of these stretch-activated chloride channels contributes to the maintenance of the nonactivated (ramified) phenotype of microglia.[32] Because AQP4 is responsible for water transport, downregulation of AQP4 through siRNA could have decreased the osmotic stress on the microglia, thus limiting the activation of the swelling-activated chloride channels, resulting in microglial activation.

Both of these mechanisms are equally possible based on the data that we report, because at 3 days, when both AQP4 levels and astrogliosis are decreased in the siAQP4-treated rats, we observed an increase in microglial activation. However, at 60 days, when AQP4 levels and extent of astrogliosis were not

Figure 7. Small-interfering RNA (siRNA) targeting aquaporin-4 (siAQP4) treatment associated with behavioral improvement at short and long term after juvenile traumatic brain injury (jTBI). siAQP4-treated pups had better functional outcomes as revealed by the foot-fault test. siAQP4 group had significantly fewer foot-faults than siGLO-treated animals at day 1 (34%) and day 3 (46%) after jTBI (*$P < 0.05$) (**A**). siAQP4 animals also performed significantly better on the rotarod test at day 3 compared with siGLO by staying on for a significantly longer time before falling (*$P < 0.05$) (**B**). After jTBI, siAQP4 treatment improves the proprioception and sensorimotor outcomes in association with a better neuronal and a decreased edema formation acutely. In Morris Water Maze (MWM) test, the groups did not show overall significant difference in the rate of spatial learning at day 1 (d1, **C**) and day 2 (d2, **D**). However, the siAQP4-treated animals exhibited higher cumulative distance value on the first block on d2 (arrows) compared with the nontreated group, suggesting a better memory of the platform's previous location. The video track (**E**, dark line) shows that the siAQP4 animals spent more time in the quadrant of platform's previous location (location noted by blue-dotted circle) than the siGLO rats, in accordance with a better memory. The actual location of the platform is noted by the red circle (**E**) and at the opposite location to the previous one. The probe test confirmed this hypothesis with a significantly higher time spent in the quadrant where the platform was located for the siAQP4-treated rats compared with the siGLO animals (**F**). All these data showed that siAQP4 treatment improves the short- and long-term behavioral outcomes. In summary (**G1** and **G2**), the primary injury induces a cascade of secondary of injuries involving AQP4 and water flow in brain tissue, which contributes to the edema formation (measured with T2 and ADC) and blood–brain barrier (BBB) disruption after jTBI. Downstream to these changes, there is neuroinflammation with astrogliosis and microglia activation, accompanied by neuronal cell death during the first days after the injury. The neuronal cell death is associated with functional impairments (**G1**). The injection the siAQP4 after jTBI (**G2**) induces a decrease in the AQP4 expression, which contributes to less entry of water and edema (measured with T2 and ADC) and also fewer constraints on the BBB. Therefore, these changes are associated with less astrogliosis and higher activation of the microglia, which could be beneficial. With these improvements, the neuronal survival is improved and accompanied by a better functional recovery after siAQP4 treatment (**G2**).

changed between the groups, no significant differences in microglial activation were observed.

Our results are in accordance with studies using knockout animals showing that AQP4$^{-/-}$ had improved outcomes compared with wild type mice in cerebral pathologies such as hyponatremia,[34] bacterial meningitis,[34] water intoxication,[25] focal cerebral ischemia,[25] spinal cord injury,[35] and encephalomyelitis.[36] Thus, the importance of the development of an AQP4 inhibitor cannot be underestimated. However, as noted earlier, no specific, effective drug directly against AQP4 is now available,[8] despite promising studies using agents such as bumetanide,[11] acetazolamide,[37,38] and methazolamide.[38,39] Our study provides a novel therapeutic strategy to successfully target AQP4, leading to better outcomes after injury when edema is a prominent pathologic feature. Our findings are unique, showing proof of concept that siAQP4 treatment when given twice after injury reduces AQP4 expression by 30% and this is sufficient to achieve beneficial functional outcomes on edema formation as well as functional improvements, even long after injury. Despite the relative modest changes in each individual measurement, the combined effect on the neurovascular unit is synergistic, with less neuronal cell death and functional improvements up to 60 days after jTBI. Furthermore, acute siAQP4 treatment does not lead to chronic or complete depletion of AQP4, which in itself could be detrimental to recovery.

Future research could be directed at investigating the most efficient method to deliver an AQP4 inhibitor to the brain without craniotomy. One potential administration route would be intranasal delivery, which bypasses the BBB, is noninvasive and easily performed.[40] Our novel findings provide compelling evidence for the effectiveness of siAQP4 as a potential therapeutic agent not only for jTBI, but also for other brain disorders in which edema is a significant contributing factor.

DISCLOSURE/CONFLICT OF INTEREST

The authors declare no conflict of interest.

ACKNOWLEDGEMENTS

The authors would like to thank Kamalakar Ambadipudi and Sonny Kim for help with MR imaging, Monica Rubalcava for assistance in the LLUSM AIM, Nina Nishiyama and Germaine Paris for assistance in immunohistochemistry.

REFERENCES

1 Faul MXL, Wald MM, Coronado VG. *Traumatic Brain Injury in the United States: Emergency Department Visits, Hospitalizations and Deaths 2002-2006.* Atlanta (GA): Centers for Disease Control and Prevention, National center for Injury Prevention and Control 2010.
2 Pop V, Badaut JA. Neurovascular perspective for long-term changes after brain trauma. *Transl Stroke Res* 2011; **2**: 533–545.
3 Moran LM, Taylor HG, Rusin J, Bangert B, Dietrich A, Nuss KE *et al.* Quality of life in pediatric mild traumatic brain injury and its relationship to postconcussive symptoms. *J Pediatr Psychol* 2012; **37**: 736–744.
4 Margulies S, Hicks R. Combination therapies for traumatic brain injury: prospective considerations. *J Neurotrauma* 2009; **26**: 925–939.
5 Ajao DO, Pop V, Kamper JE, Adami A, Rudobeck E, Huang L *et al.* Traumatic brain injury in young rats leads to progressive behavioral deficits coincident with altered tissue properties in adulthood. *J Neurotrauma* 2012; **29**: 2060–2074.
6 Fukuda AM, Pop V, Spagnoli D, Ashwal S, Obenaus A, Badaut J. Delayed increase of astrocytic aquaporin 4 after juvenile traumatic brain injury: possible role in edema resolution? *Neuroscience* 2012; **222**: 366–378.
7 Pop V, Sorensen DW, Kamper JE, Ajao DO, Murphy MP, Head E *et al.* Early brain injury alters the blood-brain barrier phenotype in parallel with beta-amyloid and cognitive changes in adulthood. *J Cereb Blood Flow Metab* 2013; **33**: 205–214.
8 Badaut J, Ashwal S, Obenaus A. Aquaporins in cerebrovascular disease: a target for treatment of brain edema? *Cerebrovasc Dis* 2011; **31**: 521–531.
9 Badaut J, Brunet JF, Regli L. Aquaporins in the brain: from aqueduct to "multi-duct". *Metab Brain Dis* 2007; **22**: 251–263.
10 Tait MJ, Saadoun S, Bell BA, Papadopoulos MC. Water movements in the brain: role of aquaporins. *Trends Neurosci* 2008; **31**: 37–43.
11 Migliati E, Meurice N, DuBois P, Fang JS, Somasekharan S, Beckett E *et al.* Inhibition of aquaporin-1 and aquaporin-4 water permeability by a derivative of the loop diuretic bumetanide acting at an internal pore-occluding binding site. *Mol Pharmacol* 2009; **76**: 105–112.
12 Igarashi H, Huber VJ, Tsujita M, Nakada T. Pretreatment with a novel aquaporin 4 inhibitor, TGN-020, significantly reduces ischemic cerebral edema. *Neurol Sci* 2011; **32**: 113–116.
13 Brower V. RNA interference advances to early-stage clinical trials. *J Natl Cancer Inst* 2010; **102**: 1459–1461.
14 Badaut J, Ashwal S, Adami A, Tone B, Recker R, Spagnoli D *et al.* Brain water mobility decreases after astrocytic aquaporin-4 inhibition using RNA interference. *J Cereb Blood Flow Metab* 2011; **31**: 819–831.
15 Badaut J, Ashwal S, Tone B, Regli L, Tian HR, Obenaus A. Temporal and regional evolution of aquaporin-4 expression and magnetic resonance imaging in a rat pup model of neonatal stroke. *Pediatr Res* 2007; **62**: 248–254.
16 Hirt L, Ternon B, Price M, Mastour N, Brunet JF, Badaut J. Protective role of early aquaporin 4 induction against postischemic edema formation. *J Cereb Blood Flow Metab* 2009; **29**: 423–433.
17 Gobbel GT, Bonfield C, Carson-Walter EB, Adelson PD. Diffuse alterations in synaptic protein expression following focal traumatic brain injury in the immature rat. *Childs Nerv Syst* 2007; **23**: 1171–1179.
18 Chastain CA, Oyoyo UE, Zipperman M, Joo E, Ashwal S, Shutter LA *et al.* Predicting outcomes of traumatic brain injury by imaging modality and injury distribution. *J Neurotrauma* 2009; **26**: 1183–1196.
19 Meng S, Qiao M, Lin L, Del Bigio MR, Tomanek B, Tuor UI. Correspondence of AQP4 expression and hypoxic-ischaemic brain oedema monitored by magnetic resonance imaging in the immature and juvenile rat. *Eur J Neurosci* 2004; **19**: 2261–2269.
20 Tourdias T, Dragonu I, Fushimi Y, Deloire MS, Boiziau C, Brochet B *et al.* Aquaporin 4 correlates with apparent diffusion coefficient and hydrocephalus severity in the rat brain: a combined MRI-histological study. *Neuroimage* 2009; **47**: 659–666.
21 Myer DJ, Gurkoff GG, Lee SM, Hovda DA, Sofroniew MV. Essential protective roles of reactive astrocytes in traumatic brain injury. *Brain* 2006; **129**: 2761–2772.
22 Berezowski V, Fukuda AM, Cecchelli R, Badaut J. Endothelial cells and astrocytes: a concerto en duo in ischemic pathophysiology. *Int J Cell Biol* 2012; **2012**: 176287.
23 Fukuda AM, Badaut J. Aquaporin 4: a player in cerebral edema and neuroinflammation. *J Neuroinflammation* 2012; **9**: 279.
24 Kimura A, Hsu M, Seldin M, Verkman AS, Scharfman HE, Binder DK. Protective role of aquaporin-4 water channels after contusion spinal cord injury. *Ann Neurol* 2010; **67**: 794–801.
25 Manley GT, Fujimura M, Ma T, Noshita N, Filiz F, Bollen AW *et al.* Aquaporin-4 deletion in mice reduces brain edema after acute water intoxication and ischemic stroke. *Nat Med* 2000; **6**: 159–163.
26 Verkman AS, Binder DK, Bloch O, Auguste K, Papadopoulos MC. Three distinct roles of aquaporin-4 in brain function revealed by knockout mice. *Biochim Biophys Acta* 2006; **1758**: 1085–1093.
27 Tait MJ, Saadoun S, Bell BA, Verkman AS, Papadopoulos MC. Increased brain edema in aqp4-null mice in an experimental model of subarachnoid hemorrhage. *Neuroscience* 2010; **167**: 60–67.
28 Shi WZ, Zhao CZ, Zhao B, Zheng XL, Fang SH, Lu YB *et al.* Aquaporin-4 deficiency attenuates acute lesions but aggravates delayed lesions and microgliosis after cryoinjury to mouse brain. *Neurosci Bull* 2012; **28**: 61–68.
29 Lu DC, Zador Z, Yao J, Fazlollahi F, Manley GT. Aquaporin-4 reduces post-traumatic seizure susceptibility by promoting astrocytic glial scar formation in mice. *J Neurotrauma* 2011, advance online publication, 22 September 2011 (e-pub ahead of print).
30 Loane DJ, Byrnes KR. Role of microglia in neurotrauma. *Neurotherapeutics* 2010; **7**: 366–377.
31 Liu W, Tang Y, Feng J. Cross talk between activation of microglia and astrocytes in pathological conditions in the central nervous system. *Life Sci* 2011; **89**: 141–146.
32 Eder C, Klee R, Heinemann U. Involvement of stretch-activated Cl- channels in ramification of murine microglia. *J Neurosci* 1998; **18**: 7127–7137.
33 Lewis RS, Ross PE, Cahalan MD. Chloride channels activated by osmotic stress in T lymphocytes. *J Gen Physiol* 1993; **101**: 801–826.
34 Papadopoulos MC, Verkman AS. Aquaporin-4 gene disruption in mice reduces brain swelling and mortality in pneumococcal meningitis. *J Biol Chem* 2005; **280**: 13906–13912.

35 Saadoun S, Bell BA, Verkman AS, Papadopoulos MC. Greatly improved neurological outcome after spinal cord compression injury in AQP4-deficient mice. *Brain* 2008; **131**: 1087–1098.
36 Li L, Zhang H, Verkman AS. Greatly attenuated experimental autoimmune encephalomyelitis in aquaporin-4 knockout mice. *BMC Neurosci* 2009; **10**: 94.
37 Huber VJ, Tsujita M, Yamazaki M, Sakimura K, Nakada T. Identification of arylsulfonamides as Aquaporin 4 inhibitors. *Bioorg Med Chem Lett* 2007; **17**: 1270–1273.
38 Tanimura Y, Hiroaki Y, Fujiyoshi Y. Acetazolamide reversibly inhibits water conduction by aquaporin-4. *J Struct Biol* 2009; **166**: 16–21.
39 Huber VJ, Tsujita M, Kwee IL, Nakada T. Inhibition of aquaporin 4 by antiepileptic drugs. *Bioorg Med Chem* 2009; **17**: 418–424.
40 Thorne RG, Hanson LR, Ross TM, Tung D, Frey 2nd WH. Delivery of interferon-beta to the monkey nervous system following intranasal administration. *Neuroscience* 2008; **152**: 785–797.